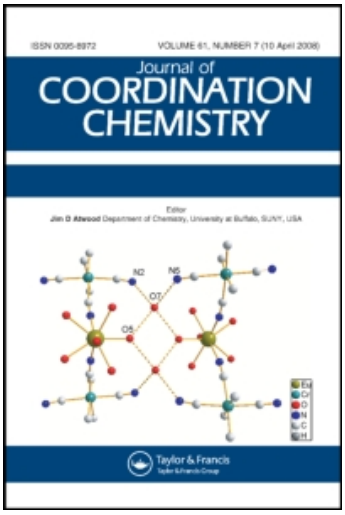

Journal of Coordination Chemistry
Publication details, including instructions for authors and subscription information:
http://www.informaworld.com/smpp/title~content=t713455674

Four benzimidazole-based Zn^{II}/Cd^{II} polymers extended by aromatic polycarboxylate coligands: synthesis, structure, and luminescence

Hong Chang[a]; Min Fu[a]; Xiao-Jun Zhao[a]; En-Cui Yang[a]
[a] College of Chemistry, Tianjin Key Laboratory of Structure and Performance for Functional Molecules, Tianjin Normal University, Tianjin 300387, P.R. China

First published on: 14 September 2010

To cite this Article Chang, Hong , Fu, Min , Zhao, Xiao-Jun and Yang, En-Cui(2010) 'Four benzimidazole-based Zn^{II}/Cd^{II} polymers extended by aromatic polycarboxylate coligands: synthesis, structure, and luminescence', Journal of Coordination Chemistry, 63: 20, 3551 — 3564, First published on: 14 September 2010 (iFirst)
To link to this Article: DOI: 10.1080/00958972.2010.515214
URL: http://dx.doi.org/10.1080/00958972.2010.515214

Journal of Coordination Chemistry
Vol. 63, No. 20, 20 October 2010, 3551–3564

Four benzimidazole-based Zn^{II}/Cd^{II} polymers extended by aromatic polycarboxylate coligands: synthesis, structure, and luminescence

HONG CHANG, MIN FU, XIAO-JUN ZHAO and EN-CUI YANG*

College of Chemistry, Tianjin Key Laboratory of Structure and Performance for Functional Molecules, Tianjin Normal University, Tianjin 300387, P.R. China

(*Received 31 March 2010; in final form 2 July 2010*)

Four benzimidazole (bim)-based metal complexes, $\{[Zn_2(bim)_4(btec)]\cdot DMF\}_n$ (**1**), $\{[Zn(bim)(btc)]\cdot Htea\}_n$ (**2**), $[Zn(bim)_2(bdc)]_n$ (**3**), and $\{[Cd_3(bim)_4(H_2O)_6(btc)_2]\cdot 2H_2O\}_n$ (**4**) ($H_4btec = 1,2,4,5$-benzenetetracarboxylic acid, $H_3btc = 1,3,5$-benzenetricarboxylic acid, $H_2bdc = 1,4$-benzenedicarboxylic acid, and tea = triethylamine), have been obtained by the introduction of benzene-based polycarboxylate as coligand and are structurally characterized by single-crystal X-ray diffraction, elemental analysis, IR spectra, thermogravimetric curves, and luminescence spectra. Controlled by the number and position of the carboxylates attached to the aromatic ring, all the four complexes exhibit polymeric structures from 1-D chain or ribbon for **1**, **3**, and **4** to 2-D layer for **2**. In contrast, the neutral bim is a terminal ligand to complete the metal coordination sphere and it also helps to assemble the low-dimensional coordination skeleton into a high-dimensional ordered supramolecular architecture by N–H···O hydrogen-bonding and π–π stacking interactions. Additionally, the complexes exhibit strong emissions originating from the bim-based intraligand as well as photo-induced interligand charge transfer upon cation binding, suggesting potential applications as luminescent materials.

Keywords: Benzimidazole; Mixed-ligand; Crystal structure; Fluorescent properties

1. Introduction

Design and construction of mixed-ligand coordination polymers has received attention due to their intriguing architectures [1] and properties, such as porosity [2], luminescence [3], magnetism [4], and catalysis [5]. Benzimidazole (bim) and its various derivatives have become promising building blocks resulting from their wide-ranging antiviral activities [6], interesting photochemical and photophysical properties [7], versatile coordination modes, and potential ability to form supramolecular aggregates through π–π stacking and hydrogen-bonding interactions [8]. Many functional metal complexes with unsubstituted bim [9–12], position isomeric pyridyl- [13–16], bi- [17], hydroxyphenyl- [18], and pyridylmethyl-benzimidazole [19] ligands as well as Zn^{II}

*Corresponding author. Email: encui_yang@yahoo.com.cn

Journal of Coordination Chemistry
ISSN 0095-8972 print/ISSN 1029-0389 online
DOI: 10.1080/00958972.2010.515214

[9–11, 13–17, 19], Cd^{II} [14, 17, 19], $Co^{II/III}$ [15, 16, 18], Cu^{II} [12, 15, 16], Mn^{II} [15], Ag^{I} [16, 20], and Hg^{II} [19] ions, have been prepared which, tuned by the nature of the metal ions and/or the ligand, have exhibited weak antiferromagnetic couplings [10] or intense luminescent emissions [12, 20]. The intriguing structures of the metal complexes may be varied or tailored by incorporating different auxiliary ligands, in which conjugated polycarboxylates are bridging ligands [21]. High-dimensional frameworks have already been generated by introducing aromatic polycarboxylate coligands in the assembly process. As continuation of the coordination behavior and luminescent property of bim, herein structurally related aromatic polycarboxylate coligands (H_4btec = 1,2,4,5-benzenetetracarboxylic acid, H_3btc = 1,3,5-benzenetricarboxylic acid, and H_2bdc = 1,4-benzenedicarboxylic acid) and Zn^{II}/Cd^{II} ions with d^{10} electron configuration were selected to assemble under controllable conditions. Four luminescent polymers, $\{[Zn_2(bim)_4(btec)]\cdot DMF\}_n$ (**1**), $\{[Zn(bim)(btc)]\cdot Htea\}_n$ (**2**), $[Zn(bim)_2(bdc)]_n$ (**3**), and $\{[Cd_3(bim)_4(H_2O)_6(btc)_2]\cdot 2H_2O\}_n$ (**4**), were isolated and fully characterized. Structural analyses reveal that **1**, **3**, and **4** are infinite 1-D ribbon/chains and **2** exhibits a 2-D Zn^{II}-btc^{3-} layer. Obviously, the polymeric nature is tuned by the binding mode, the number, and position of the polycarboxylate attached on the aromatic ring; bim is a terminal ligand to complete the metal coordination sphere. Thermal stability and intense luminescent properties were also investigated.

2. Experimental

2.1. *Materials and instruments*

All solvents and reagents were of reagent grade, commercially available and used without purification. Doubly deionized water was used for conventional synthesis. Elemental analyses for C, H, and N were performed on a CE-440 (Leeman-Labs) analyzer. Fourier transform (FT) IR spectra (KBr pellets) were taken on an Avatar-370 (Nicolet) spectrometer from 4000 to 400 cm^{-1}. Thermogravimetric analyses (TGA) were carried out on a Shimadzu simultaneous DTG-60A compositional analysis instrument from room temperature to 800°C under N_2 at a heating rate of 5°C min^{-1}. Fluorescence spectra of the complexes in acetonitrile were performed on a Cary Eclipse fluorescence spectrophotometer (Varian) at room temperature.

2.2. *Preparation of $\{[Zn_2(bim)_4(btec)]\cdot DMF\}_n$ (1)*

To an aqueous solution (5 mL) of $ZnCl_2$ (13.6 mg, 0.1 mmol), a mixed methanol-DMF solution (1 : 1, 10 mL) containing bim (11.8 mg, 0.1 mmol) and H_4btec (25.4 mg, 0.1 mmol) was slowly added with constant stirring. The resulting mixture was further stirred for 1 h and filtered. Upon slow evaporation of the filtrate at room temperature, colorless block-shaped crystals suitable for X-ray diffraction were collected within a week (Yield: 43% based on bim). Anal. Calcd for $C_{10}H_{7.50}N_{2.25}O_{2.25}Zn_{0.50}$: C, 52.71%; H, 3.32%; N, 13.83%. Found: C, 52.91%; H, 3.14%; N, 13.62%. IR (KBr, cm^{-1}): 3111 w, 1678 s, 1591 s, 1493 s, 1421 s, 1390 s, 1306 w, 747 m.

2.3. *Preparation of $\{[Zn(bim)(btc)]\cdot Htea\}_n$ (2)*

To an aqueous solution (3 mL) of $ZnCl_2$ (13.6 mg, 0.1 mmol), a methanol solution (7 mL) containing bim (11.8 mg, 0.1 mmol) and H_3btc (21.0 mg, 0.1 mmol) was slowly added with constant stirring. The pH of the mixture was adjusted to 7 by triethylamine. After further stirring for 1 h, the resulting mixture was filtered. Upon slow evaporation of the filtrate at room temperature, blue block-shaped crystals were grown within 10 days (Yield: 58% based on bim). Anal. Calcd for $C_{22}H_{25}N_3O_6Zn$: C, 53.62%; H, 5.11%; N, 8.53%. Found: C, 53.75%; H, 4.99%; N, 8.53%. IR (KBr, cm^{-1}): 3113 w, 1623 s, 1564 s, 1421 m, 1368 s, 1344 s, 1306 m, 649 w, 722 m.

2.4. *Preparation of $[Zn(bim)_2(bdc)]_n$ (3)*

$Zn(OAc)_2\cdot 3H_2O$ (21.9 mg, 0.1 mmol), bim (11.8 mg, 0.1 mmol), H_2bdc (16.6 mg, 0.1 mmol), doubly deionized water (10 mL), and NaOH solution (0.2 mol L^{-1}, 0.5 mL) were sealed in a Teflon-lined reactor (23 mL) and heated at 140°C for 72 h. After cooling to room temperature at a rate of 2.5°C h^{-1}, the resulting mixture was filtered. The filtrate was left under ambient environment for slow evaporation. Colorless block-shaped crystals suitable for X-ray diffraction were obtained within 7 days (Yield: 41% based on bim). Anal. Calcd for $C_{22}H_{16}N_4O_4Zn$: C, 56.73%; H, 3.46%; N, 12.03%. Found: C, 56.67%; H, 3.46%; N, 12.14%. IR (KBr, cm^{-1}): 3136 w, 1595 s, 1500 s, 1409 m, 1352 vs, 1277 w, 1251 w, 834 w, 744 s.

2.5. *Preparation of $\{[Cd_3(bim)_4(H_2O)_6(btc)_2]\cdot 2H_2O\}_n$ (4)*

Complex **4** was achieved under hydrothermal conditions. $Cd(OAc)_2\cdot 4H_2O$ (26.7 mg, 0.1 mmol), bim (11.8 mg, 0.1 mmol), H_3btc (21.0 mg, 0.1 mmol), and doubly deionized water (10 mL) were sealed in a Teflon-lined reactor (23 mL) and the pH adjusted to 7 with NaOH solution (0.2 mol L^{-1}). After being heated at 140°C for 72 h, the resulting mixture was cooled to room temperature and filtered. Pale yellow block-shaped crystals suitable for X-ray diffraction analysis were obtained within 7 days by slow evaporation of the filtrate (Yield: 55% based on bim). Anal. Calcd for $C_{23}H_{23}N_4O_{10}Cd_{1.50}$: C, 40.38%; H, 3.39%; N, 8.19%. Found: C, 40.34%; H, 3.26%; N, 8.32%. IR (KBr, cm^{-1}): 3136 w, 1595 vs, 1501 s, 1422 s, 1386 s, 1351 s, 1302 m, 1278 m, 1253 m, 975 w, 834 w, 778 w, 745 s.

2.6. *X-ray crystallography*

Single-crystal X-ray diffraction studies of **1**–**4** were performed on a Bruker Apex II CCD diffractometer equipped with graphite monochromated Mo-Kα radiation with radiation wavelength 0.71073 Å using the φ–ω scan mode at 296(2) K. There was no evidence of crystal decay during data collection. The multi-scan absorption correction was carried out for all the data by SADABS. SAINT [22] was used for integration of the diffraction profiles. All structures were solved by direct methods using SHELXS program of the SHELXTL-97 package and refined with SHELXL [23]. The final refinement was performed by full-matrix least-squares methods on F^2 with anisotropic thermal parameters for all non-hydrogen atoms. The positions of hydrogens bonded to

carbon were generated geometrically and allowed to ride on their parent carbons before the final cycle of refinement. Hydrogens attached to oxygen were first located in difference Fourier maps and then placed in calculated sites, and refined isotropically. In **1**, lattice DMF shows dynamic disorder and the site occupancy for the disorder C(11), C(12), O(4), and N(3) is 0.5. Further crystallographic data and experimental details for structural analysis of **1**–**4** are summarized in table 1. The selected bond distances and angles are shown in table 2 and the hydrogen bond parameters are listed in table 3.

3. Results and discussion

3.1. *Synthesis and IR spectra*

Crystallization of metal complexes is affected by factors including temperature, solvent, preparation method, etc. Herein, **1** and **2** were obtained by the conventional evaporation method in mixed methanol-DMF for **1** and in methanol–water for **2**. In contrast, **3** and **4** were isolated under hydrothermal conditions by controlling the cooling rate of the reaction mixture. Although the number of carboxylate groups in coligands is different, the molar ratio of the reactants in the four complexes is 1 : 1 : 1 (Zn^{II}/Cd^{II} : bim : aromatic acid). The pH value is also a key factor for construction of the target complexes, since the deprotonated behavior of the aromatic acid is sensitive to pH. Full deprotonations of the aromatic acids were observed for **1**–**4**.

In IR spectra, weak absorptions at 3111 cm^{-1} for **1**, 3113 cm^{-1} for **2**, and 3136 cm^{-1} for both **3** and **4** can be assigned to ν(N–H) and/or ν(C–H) of bim [17, 19]. The strong band at 1678 cm^{-1} in **1** should be associated with $\nu_{C=O}$ of DMF. The absence of the band at *ca* 1700 cm^{-1} in **1**–**4** suggests full deprotonation of aromatic acids in all the complexes. Correspondingly, the strong asymmetric (ν_{as}) and symmetric vibrations (ν_s) of the carboxylate groups are located at 1591 and 1390 cm^{-1} for **1**, 1623 and 1368 cm^{-1} for **2**, 1595 and 1352 cm^{-1} for **3** as well as 1595, 1501, 1422, and 1386 cm^{-1} for **4**, respectively. The differences between ν_{as} and ν_s ($\Delta\nu = \nu_{as} - \nu_s = 201$, 255, and 243 cm^{-1} for **1**–**3**, respectively) indicate unidentate coordination of carboxylate [24]. The $\Delta\nu$ values (79 and 209 cm^{-1}) for **4** indicate bidentate and unidentate carboxylate, which can also be confirmed by single-crystal structure determinations. Skeleton vibrations of the aromatic or hetero-aromatic ring can be observed at 1600–1400 cm^{-1} [24].

3.2. *Structural description of {[Zn$_2$(bim)$_4$(btec)]·DMF}$_n$ (1)*

Single-crystal X-ray diffraction analysis reveals that **1** exhibits a 1-D linear ribbon extended by centrosymmetric $btec^{4-}$. As shown in figure 1(a), the crystallographically independent Zn^{II} is coordinated by two N from two different bim and two carboxylates from two symmetry-related $btec^{4-}$ linkers, leading to deformed tetrahedral coordination. The Zn–N distance is slightly longer than that of Zn–O (table 2), comparable to previous values [9–11, 13–17, 19].

The $btec^{4-}$ presents a μ_4–κ^1O1 : κ^1O4 : κ^1O6 : κ^1O8 coordination mode to link four symmetry-related Zn^{II} ions into an infinite 1-D polymeric ribbon along the crystallographic *c*-axis, with two separate bim ligands terminally coordinated to one Zn^{II} to complete the coordinate sphere (figure 1b). The bim presented as protonated N–H

Table 1. Crystal data and structure refinement for **1**–**4**.

	1	**2**	**3**	**4**
Empirical formula	$C_{10}H_{7.50}N_{2.25}O_{2.25}Zn_{0.50}$	$C_{22}H_{25}N_3O_6Zn$	$C_{22}H_{16}N_4O_4Zn$	$C_{23}H_{23}N_4O_{10}Cd_{1.50}$
Formula weight ($g\,mol^{-1}$)	227.87	492.82	465.76	684.05
Crystal system	Monoclinic	Orthorhombic	Monoclinic	Triclinic
Space group	$C2/m$	$Pbca$	$P2_1/n$	$P\bar{1}$
Unit cell dimensions (Å, °)				
a	14.4727(6)	13.9626(5)	17.3685(18)	10.2458(4)
b	18.8288(8)	16.2685(6)	7.2012(7)	10.5562(4)
c	7.7997(3)	19.2912(8)	17.8572(17)	13.1060(5)
α	90	90	90	70.9210(10)
β	110.1910(10)	90	114.756(2)	74.4520(10)
γ	90	90	90	85.1680(10)
Volume ($Å^3$), Z	1994.83(14), 8	4382.0(3), 8	2028.2(3), 4	1290.6(9), 2
Calculated density ($g\,cm^{-3}$)	1.517	1.494	1.525	1.760
Absorption coefficient (mm^{-1})	1.270	1.165	1.249	1.310
$F(0\,0\,0)$	930	2048	952	682
Crystal size (mm^3)	$0.22 \times 0.20 \times 0.18$	$0.24 \times 0.22 \times 0.20$	$0.24 \times 0.23 \times 0.22$	$0.25 \times 0.24 \times 0.15$
Limiting indices	$-12 \le h \le 17$; $-21 \le k \le 22$; $-9 \le l \le 8$	$-16 \le h \le 15$; $-19 \le k \le 11$; $-22 \le l \le 22$	$-20 \le h \le 20$; $-8 \le k \le 8$; $-9 \le l \le 21$	$-12 \le h \le 11$; $-12 \le k \le 11$; $-15 \le l \le 10$
Reflections collected	5129	21089	9900	6622
Independent reflection	1830 [R(int) = 0.0161]	3844 [R(int) = 0.0340]	3585 [R(int) = 0.0341]	4523 [R(int) = 0.0132]
Max. and min. transmission	0.8036 and 0.7675	0.7836 and 0.7673	0.7707 and 0.7537	0.8278 and 0.7354
Data/restraints/parameters	1830/4/154	3844/15/292	3585/0/280	4523/0/349
Goodness-of-fit on F^2	1.071	1.031	1.054	1.046
Final R indices [$I > 2\sigma(I)$][a]	$R_1 = 0.0309$, $wR_2 = 0.0947$	$R_1 = 0.0337$, $wR_2 = 0.0800$	$R_1 = 0.0333$, $wR_2 = 0.0737$	$R_1 = 0.0205$, $wR_2 = 0.0529$
R indices (all data)	$R_1 = 0.0325$, $wR_2 = 0.0959$	$R_1 = 0.0466$, $wR_2 = 0.0874$	$R_1 = 0.0501$, $wR_2 = 0.0800$	$R_1 = 0.0222$, $wR_2 = 0.0541$
Largest difference peak and hole (e $Å^{-3}$)	0.639 and −0.248	0.826 and −0.417	0.244 and −0.299	0.366 and −0.667

[a] $R_1 = \Sigma||F_o| - |F_c||/|F_o|$; $wR_2 = [\Sigma w(F_o^2 - F_c^2)^2/\Sigma w(F_o^2)^2]^{1/2}$.

Table 2. Selected bond lengths (Å) and angles (°) for **1**–**4**.

1			
Zn(1)–N(1)	1.99(2)	Zn(1)–O(1)	1.93(17)
O(1)[a]–Zn(1)–O(1)	95.23(1)	N(1)[a]–Zn(1)–N(1)	106.90(1)
O(1)–Zn(1)–N(1)[a]	118.54(8)	O(1)–Zn(1)–N(1)	108.97(9)
2			
Zn(1)–O(1)	1.96(2)	Zn(1)–O(6)[a]	1.97(2)
Zn(1)–O(3)[b]	1.98(2)	Zn(1)–N(1)	2.02(2)
O(1)–Zn(1)–O(6)[a]	109.63(9)	O(1)–Zn(1)–O(3)[b]	113.05(9)
O(6)[a]–Zn(1)–O(3)[b]	104.87(9)	O(1)–Zn(1)–N(1)	112.71(1)
O(6)[a]–Zn(1)–N(1)	113.48(9)	O(3)[b]–Zn(1)–N(1)	102.74(1)
3			
Zn(1)–O(3)	1.98(2)	Zn(1)–O(1)	2.02(2)
Zn(1)–N(3)	2.02(2)	Zn(1)–N(1)	2.03(2)
O(3)–Zn(1)–O(1)	107.64(8)	O(3)–Zn(1)–N(3)	102.65(8)
O(1)–Zn(1)–N(3)	110.15(9)	O(3)–Zn(1)–N(1)	107.65(9)
O(1)–Zn(1)–N(1)	117.49(9)	N(3)–Zn(1)–N(1)	110.14(10)
4			
Cd(1)–O(4)	2.20(2)	Cd(1)–O(9)	2.33(2)
Cd(1)–O(8)	2.32(2)	Cd(2)–O(5)[b]	2.40(2)
Cd(2)–N(3)	2.29(2)	Cd(2)–N(1)	2.29(2)
Cd(2)–O(2)	2.32(1)	Cd(2)–O(7)	2.33(2)
Cd(2)–O(6)[b]	2.45(2)		
O(4)–Cd(1)–O(4)[a]	180.0	O(4)–Cd(1)–O(8)[a]	87.26(6)
O(9)[a]–Cd(1)–O(9)	180.00(9)	O(4)–Cd(1)–O(8)	92.74(6)
O(4)–Cd(1)–O(9)[a]	93.30(7)	O(4)–Cd(1)–O(9)	86.70(7)
O(8)–Cd(1)–O(9)	89.91(7)	N(3)–Cd(2)–N(1)	94.47(7)
O(8)–Cd(1)–O(9)[a]	90.09(7)	O(5)[b]–Cd(2)–O(6)[b]	53.39(5)
N(3)–Cd(2)–O(2)	88.50(6)	N(1)–Cd(2)–O(2)	141.03(6)
N(3)–Cd(2)–O(7)	162.53(6)	N(1)–Cd(2)–O(7)	87.43(6)
O(2)–Cd(2)–O(7)	79.30(6)	N(3)–Cd(2)–O(5)[b]	100.28(7)
N(1)–Cd(2)–O(5)[b]	134.25(6)	O(2)–Cd(2)–O(5)[b]	82.79(5)
O(7)–Cd(2)–O(5)[b]	90.63(6)	N(3)–Cd(2)–O(6)[b]	105.37(7)
N(1)–Cd(2)–O(6)[b]	80.99(6)	O(2)–Cd(2)–O(6)[b]	135.43(5)
O(7)–Cd(2)–O(6)[b]	92.08(6)		

Symmetry codes for **1**: [a] $-x, y, -z$; **2**: [a] $x-1/2, 1/2-y, 1-z$; [b] $x-1/2, y, 3/2-z$; **4**: [a] $1-x, -y-1, 1-z$; [b] $x+1, y, z$.

hydrogen-bonding donor can also produce N2–H2 $\cdots$ O2 interaction with the carboxylate of $btec^{4-}$, assembling adjacent ribbons into a 3-D supramolecular network (table 3 and figure 1c). A complex similar to **1**, $\{[Zn_2(bim)_4(btec)]\cdot H_2O\}_n$ [11], was prepared under hydrothermal conditions, crystallizing in monoclinic $C2/c$ space group, not the $C2/m$. Although the bonding modes of both ligands and the coordination polyhedron of Zn^{II} are the same, the spatial orientation of bim is obviously different. The dihedral angle between the two bim planes is 80.358° in **1**, much larger than that of $\{[Zn_2(bim)_4(btec)]\cdot H_2O\}_n$ (49.24(6)°). Thus, the high-dimensional supramolecular structure of **1** is formed by hydrogen-bonding interactions rather than π–π stacking interactions.

3.3. *Structural description of* $\{[Zn(bim)(btc)]\cdot Htea\}_n$ *(2)*

Complex **2** consists of an anionic Zn^{II}-btc^{3-} layer and a cationic triethylamine for charge compensation. Although the Zn^{II} in the asymmetric unit of **2** is also in a

Table 3. Hydrogen-bonding parameters (Å, °) for **1**–**4**.

Donor–H···Acceptor	*d*(H···A)	*d*(D···A)	∠(D–H···A)
1			
N2–H2···O2[a]	2.03	2.799(3)	148
2			
N2–H2···O4[a]	1.97	2.762(3)	152
N3–H3A···O5[b]	1.82	2.713(4)	168
3			
N4–H4′···O1[a]	2.08	2.812(3)	143
N2–H2′···O4[b]	1.94	2.732(3)	152
4			
O7–H7A···O3[a]	1.84	2.672(2)	167
N4–H4′···O1[b]	1.93	2.781(3)	169
O8–H8B···O1[c]	2.04	2.885(2)	169
O9–H9A···O6[c]	1.90	2.746(3)	175
O10–H10A···O2[a]	1.95	2.743(2)	155
O10–H10B···O5[d]	2.22	2.789(3)	126
N2–H2′···O10	2.01	2.855(3)	168
O7–H7B···O10[e]	2.02	2.831(2)	158

Symmetry codes for **1**: [a] $1/2+x, 1/2-y, 1+z$; **2**: [a] $2-x, -1/2+y, 3/2-z$; [b] $-1+x, y, z$; **3**: [a] $x, 1+y, z$; [b] $-x, -y, -z$; **4**: [a] $2-x, 1-y, -z$; [b] $2-x, -y, 1-z$; [c] $x, -1+y, z$; [d] $1-x, -y, 1-z$; [e] $2-x, 1-y, 1-z$.

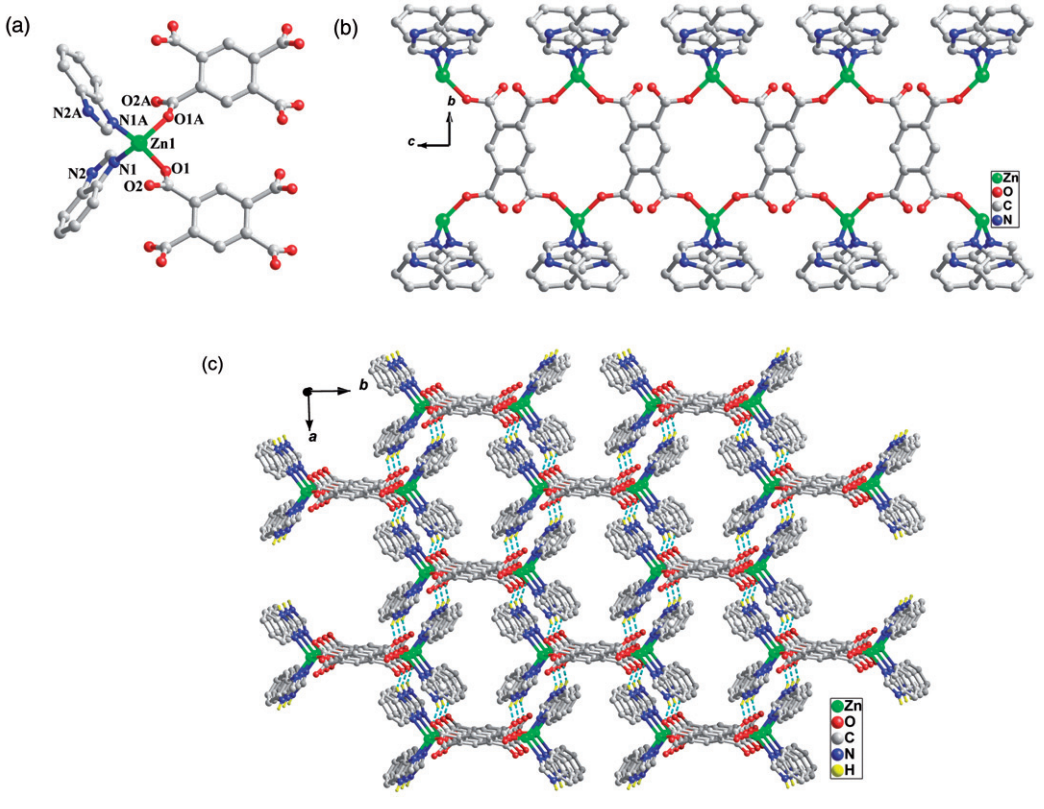

Figure 1. (a) Local coordination environment of Zn^{II} in **1** (hydrogens were omitted for clarity, symmetry codes: $A = -x, y, 1-z$). (b) View of 1-D ribbon of **1** extended by $btec^{4-}$. (c) 3-D hydrogen-bonded supramolecular network of **1**.

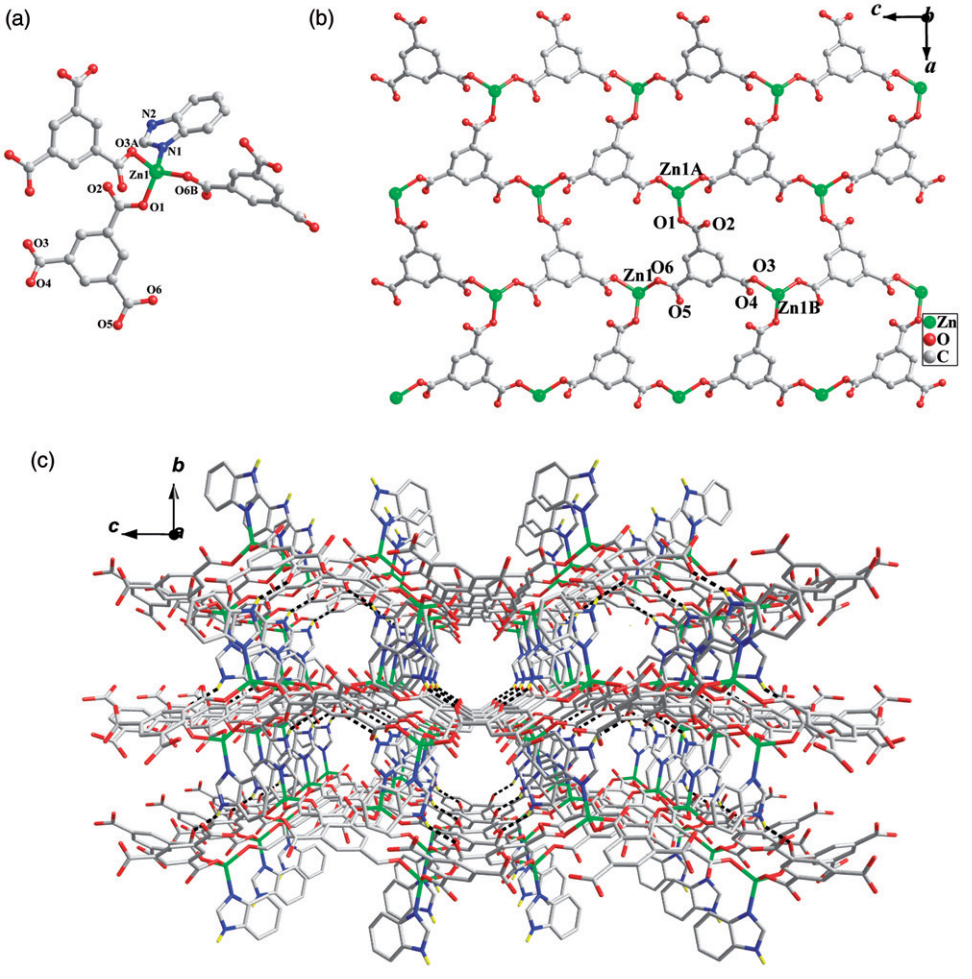

Figure 2. (a) Local coordination environment of Zn^{II} in **2** (hydrogens were omitted for clarity, symmetry codes: A = $x-0.5$, y, $1.5-z$; B = $x-0.5$, $0.5-y$, $1-z$). (b) 2-D sheet of **2** composed of 24-membered Zn^{II}-btc^{3-} macrocycles (symmetry codes: A = $x-0.5$, $0.5-y$, $1-z$; B = x, $0.5-y$, $z-0.5$). (c) 3-D hydrogen-bonded supramolecular network of **2**.

distorted tetrahedron (figure 2a), the coordination environment of the metal ion is slightly different from that in **1**. Each Zn^{II} in **2** is surrounded by one N from a neutral bim and three carboxylates from three separate btc^{3-}. The distances and angles around Zn^{II} (table 2) are comparable to **1** and reported values [9–11, 13–17, 19].

The fully deprotonated btc^{3-} in **2** adopts a μ_3–κ^1O1 : κ^1O3 : κ^1O6 coordination mode to connect three symmetry-related Zn^{II} ions into a 2-D layer in the crystallographic *ac* plane (figure 2b). The 2-D layer is made of 24-membered Zn^{II}-btc^{3-} macrocycles. Further analysis indicates that the adjacent Zn^{II}-COO^- chains within the 2-D layers alternate left- and right-handed helices, making the overall layered structure of **2** racemic.

Adjacent layers were further connected by non-covalent N2–H2···O4 interactions between N–H of imidazole and carboxylate of btc^{3-}, leading to a 3-D supramolecular

network (figure 2c). Protonated triethylamine molecules are entrapped in the 3-D supramolecular network through N3–H3A···O5 hydrogen-bonding interactions (table 3 and figure S1).

3.4. *Structural description of $[Zn(bim)_2(bdc)]_n$ (3)*

As shown in figure 3(a), **3** possesses a 1-D *zigzag* chain bridged by fully deprotonated bdc^{2-}. One Zn^{II} ion, two different bim ligands, and one bdc^{2-} ligand exist in the asymmetric unit. The Zn^{II} in **3** is also in a distorted tetrahedron constructed by pairs of N donors from two separate bim ligands and two carboxylate oxygens from two head-to-tail arranged bdc^{2-}. The bdc^{2-} is bis-monodentate bridging to aggregate adjacent Zn^{II} ions into a *zigzag* chain along [1 0 1], with a pair of terminal bim ligands to complete the Zn^{II} coordination. The Zn···Zn distance separated by bridged bdc^{2-} is 10.9146(8)° Å and the angle of the three adjacent Zn^{II} atoms is 120.949(4)°.

The adjacent *zigzag* chains are further connected into a 2-D sheet by N4–H4′···O1 hydrogen-bonding interaction (figure 3b). Adjacent layers are stacked by alternate π–π stacking and N2–H2′···O4 hydrogen-bonding interactions (figure 3c). The centroid–centroid distance and the dihedral angle between the benzimidazole ring system involved in the π–π stacking interaction is 3.686 Å and 0.0°, respectively.

3.5. *Structural description of $\{[Cd_3(bim)_4(H_2O)_6(btc)_2]\cdot 2H_2O\}_n$ (4)*

Possessing the same ligands (bim and btc^{3-}) as **2**, complex **4** is a ladder-like 1-D polymer. The asymmetric unit of **4** contains one and a half Cd^{II}, a pair of terminal bim ligands, one completely deprotonated btc^{3-}, and four water molecules (three coordinated and the other lattice). Cd1 atom, located at the inversion center, is six-coordinate by four water molecules in the equatorial plane and two symmetry-related monodentate carboxylates of two btc^{3-} ligands occupying axial positions in distorted octahedral coordination (table 2). In contrast, Cd2 is seven coordinate to four carboxylate oxygens from two btc^{3-} ligands, two imidazole N donors from two separate bim ligands, and one coordinated water molecule. The coordination geometry around each Cd2 is distorted pentagonal-bipyramidal, in which Cd^{II} deviates from the least-squares plane generated by O1–O2–O5–O6–N1 by 0.2046 Å. Cd–O bonds fall in the range 2.2040(15)–2.4545(15) Å and bond angles around each Cd^{II} are 53.39(5)°–180.0° (table 2).

Rather than being monodentate as in **2**, the three carboxylates of btc^{3-} in **4** adopt two different binding modes, which link adjacent Cd2 in a bidentate chelating mode along the crystallographic *a*-direction and connect Cd1 and Cd2 in a monodentate manner along the crystallographic *b*-axis. As a result, a 1-D ribbon-like molecular ladder with terminal bim as brims is generated (figure 4a).

Due to the presence of various coordinated water molecules and protonated N–H on bim as hydrogen-bonding donors, the molecular ladders are H-bonded together with the carboxylate group of btc^{3-} (table 3) and a 3-D supramolecular architecture was generated (figure 4b), in which lattice water molecules were entrapped by O–H···O and N–H···O hydrogen-bonding interactions (table 3).

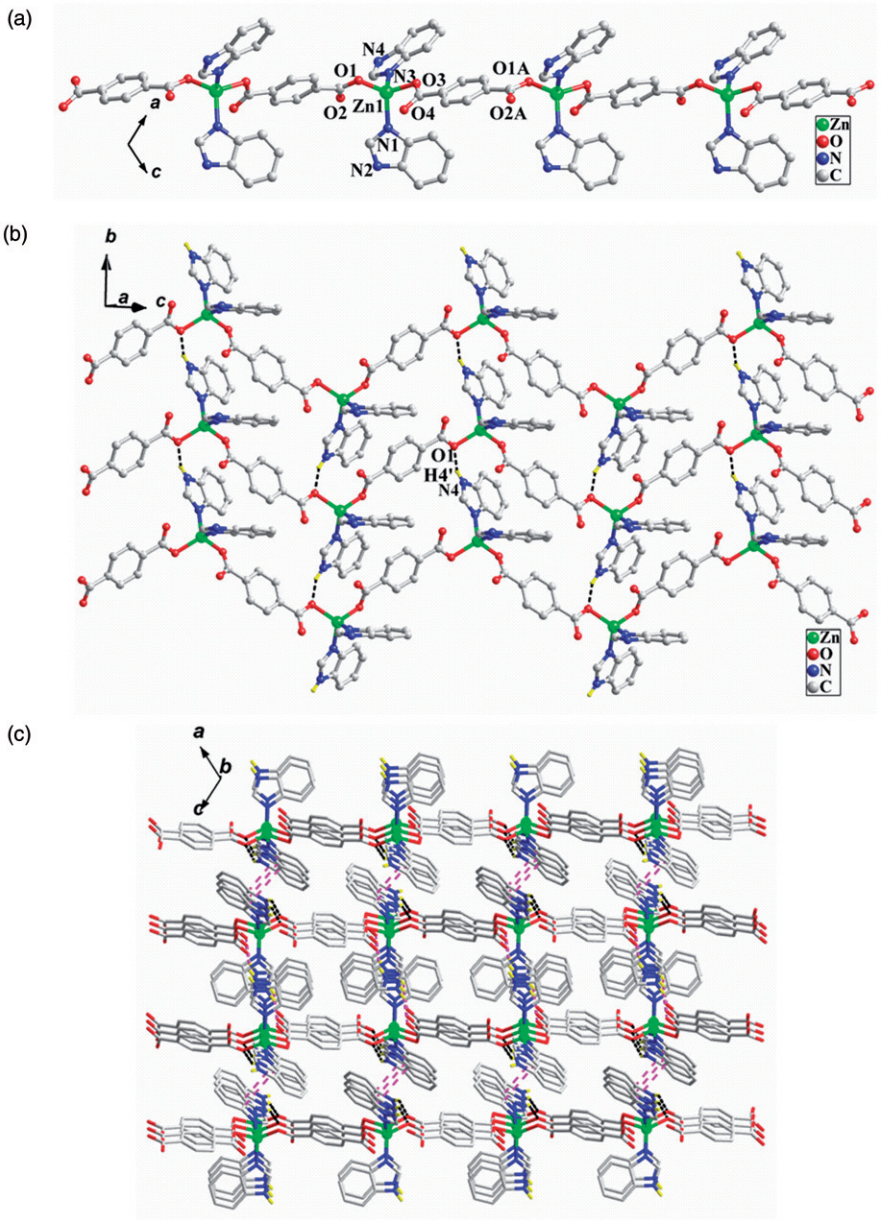

Figure 3. (a) An infinite chain of **3** linked by bdc^{2-} with the atomic labels in the asymmetric unit. (b) 2-D layer of **3** formed by N–H $\cdots$ O hydrogen-bonding interactions. (c) 3-D supramolecular network of **3** formed by alternate N–H $\cdots$ O hydrogen-bonding and $\pi \cdots \pi$ stacking interactions.

3.6. *Thermal stability of 1–4*

TG experiments of the complexes were performed from room temperature to 800°C to explore the thermal stability of **1–4** (figure 5). Complex **1** showed thermal instability above 144°C with lattice DMF, coordinated bim and $btec^{4-}$ continuously lost between

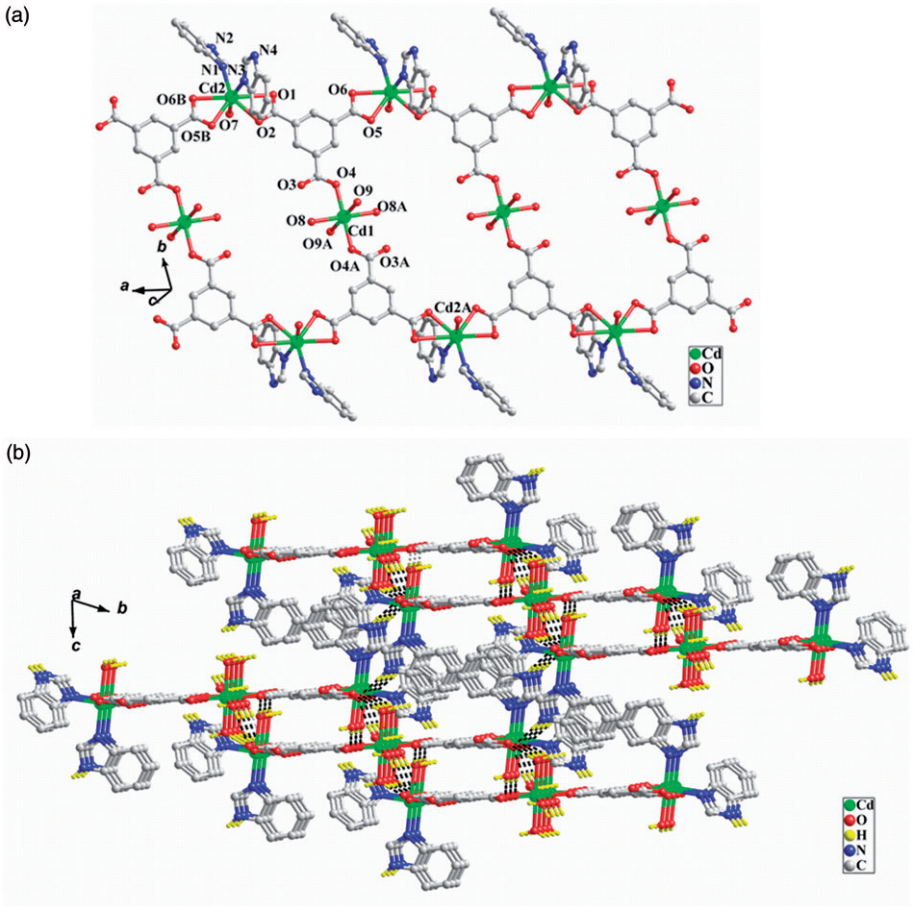

Figure 4. (a) View of 1-D ribbon of **4** with the atomic labels in the asymmetric unit (hydrogens were omitted for clarity, symmetry codes: $A = 1 - x, -1 - y, 1 - z$). (b) 3-D network of **4** formed by extensive hydrogen-bonding interactions.

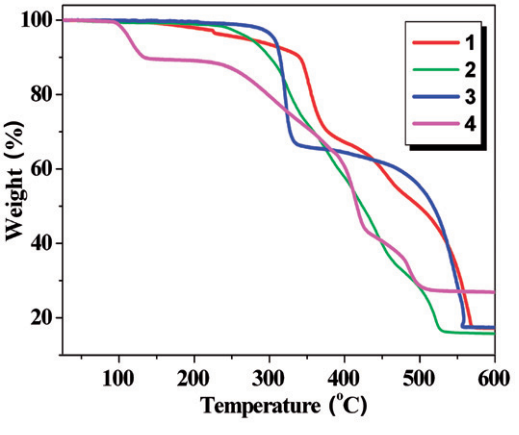

Figure 5. TG curves for **1**–**4**.

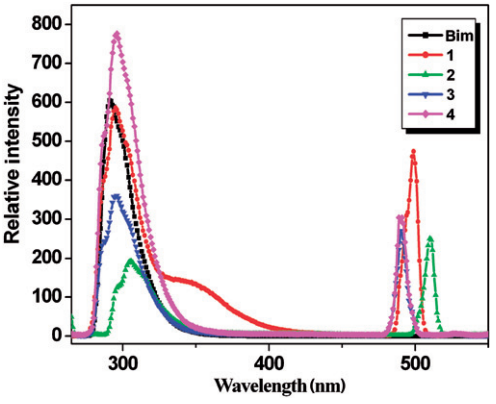

Figure 6. Emission spectra for **1–4** in acetonitrile at room temperature.

144°C and 575°C (obsd 82.4%, Calcd 82.1%), leaving ZnO as final product (obsd 17.6%, Calcd 17.9%). Similar to **1**, **2** also exhibited a one-stage weight loss (obsd 84.0%, Calcd 83.5%) for removal of protonated $Htea^{+}$, coordinated bim, and btc^{3-} beginning at 232°C and ending at 535°C. Thus, **2** is more stable than **1**. In contrast, both **3** and **4** displayed two separate weight loss processes, suggesting different thermal behavior. For **3** without any lattice molecules, bim and bdc^{2-} decomposed successively in a first stage from 268°C to 342°C for bdc^{2-} (obsd 32.6%, Calcd 31.8%) and the second from 342°C to 563°C for bim (obsd 51.4%, Calcd 50.7%); the final product above 563°C was ZnO (obsd 17.8%, Calcd 17.5%). The lattice water molecules of **4** were released between 93°C and 142°C (10.9% weight loss, Calcd 10.5%). The ligands of **4** decomposed between 142°C and 519°C and the final residue was CdO (obsd 27.7%, Calcd 28.1%).

3.7. *Luminescence*

Free bim can display emissions due to its localized aromatic skeleton and various electronic energy levels [25, 26]. As shown in figure 6, the four complexes display a strong emission at *ca* 300 nm and a relatively weak emission at *ca* 500 nm in acetonitrile at room temperature. To explore the nature of these emissions, luminescence spectra of isolated bim, H_4btec, H_3btc, and H_2bdc were also measured under comparable experimental conditions; only one strong emission at 300 nm was observed from the $\pi \rightarrow \pi^*$ charge transfer of bim [27]. The aromatic acids are non-luminescent in the range 250–600 nm. Thus, strong emissions of the complexes at high frequency should be ascribed to bim-based intraligand $\pi \rightarrow \pi^*$ charge transfer and the new emissions are probably due to the photo-induced interligand charge transfer upon cation binding [28, 29], since the d^{10} Zn^{II} and Cd^{II} have no empty d orbital for excess electrons.

4. Conclusion

Four bim-based luminescent Zn^{II}/Cd^{II} polymers with 1-D chain/ribbon or 2-D layer were isolated by incorporating aromatic polycarboxylate coligands. These extended

coordination frameworks were tuned by the bridging carboxylate rather than the terminal bim. Hydrogen-bonding interaction involving the N–H donor of bim dominates the high-dimensional ordered supramolecular network. Additionally, upon cation binding, the four complexes display strong emissions, suggesting potential applications as luminescent materials.

Supplementary material

Crystallographic data (excluding structure factors) for the crystal structures reported in this article have been deposited with the Cambridge Crystallographic Data Center (CCDC nos. 736933–736936). This material can be obtained free of charge *via* www.ccdc.cam.ac.uk/conts/retrieving.html or from the CCDC, 12 Union Road, Cambridge CB2 1EZ, UK; Fax: (+44) 1223 336033; Email: deposit@ccdc.cam.ac.uk.

Acknowledgments

This study was financially supported by the Key Project of Chinese Ministry of Education (grant no. 209003), the Program for New Century Excellent Talents in University (NCET-08-0914), the Natural Science Foundation of Tianjin (grant nos. 10JCZDJC21600 and 10JCYBJC04800) and the Academic Advance Project for Young Teachers of Tianjin Normal University, which are gratefully acknowledged.

References

[1] (a) H. Malcolm. *Coord. Chem. Rev.*, **21**, 2493 (2009); (b) D. Maspoch, D. Ruiz-Molina, J. Veciana. *J. Mater. Chem.*, **14**, 2713 (2004); (c) S.R. Batten, K.S. Murray. *Coord. Chem. Rev.*, **246**, 103 (2003); (d) L. Carlucci, G. Ciani, D. Proserpio. *Coord.Chem. Rev.*, **246**, 247 (2003).
[2] (a) J.J. Perry IV, J.A. Perman, M.J. Zaworotko. *Chem. Soc. Rev.*, **38**, 1400 (2009); (b) G.K.H. Shimizu, R. Vaidhyanathan, J.M. Taylor. *Chem. Soc. Rev.*, **38**, 1430 (2009); (c) X. He, C.-Z. Lu, D.-Q. Yuan. *Inorg. Chem.*, **45**, 5760 (2006); (d) H. Deng, Y.-C. Qiu, Y.-H. Li, Z.-H. Liu, R.-H. Zeng. *Chem. Commun.*, 2239 (2008).
[3] A. Barbieri, G. Accorsi, N. Armaroli. *Chem. Commun.*, 2185 (2008).
[4] (a) R. Sessoli, A.K. Powell. *Coord. Chem. Rev.*, **19**, 2328 (2009); (b) V. Lozan, C. Loose, J. Kortus, B. Kersting. *Coord. Chem. Rev.*, **19**, 2244 (2009).
[5] (a) H. Kozlowski, A. Janick-Klos, J. Brasun, E. Gaggelli, D. Valensin, G. Valensin. *Coord. Chem. Rev.*, **253**, 2665 (2009); (b) R.H. Morris. *Chem. Soc. Rev.*, **38**, 2282 (2009).
[6] R.R. Tidwell, S.K. Jones, N.A. Naiman, L.C. Berger, W.B. Brake, C.C. Dykstra, J.E. Hall. *Antimicrob. Agents Chemother.*, **37**, 1713 (1993).
[7] S. Santra, S.K. Dogra. *J. Mol. Struct.*, **476**, 223 (1999).
[8] (a) C.-Y. Su, B.-S. Kang, Q.-C. Yang, T.C.W. Mak. *J. Chem. Soc., Dalton Trans.*, 1857 (2000); (b) C.J. Matthews, V. Broughton, G. Bernardinelli, X. Melich, G. Brand, A.C. Willis, A.F. Williams. *New J. Chem.*, **27**, 354 (2003); (c) D. Moon, M.S. Lah, R.E.D. Sesto, J.S. Miller. *Inorg. Chem.*, **41**, 4708 (2002); (d) B.S. Hammes, M.T. Kieber-Emmons, R. Sommer, A.L. Rheingold. *Inorg. Chem.*, **41**, 1351 (2002).
[9] (a) E. Sahin, S. Ide, M. Kurt, S. Yurdakul. *Z. Kristallogr.*, **218**, 385 (2003); (b) X.-C. Huang, J.-P. Zhang, X.-M. Chen. *Chin. Sci. Bull.*, **14**, 1491 (2003); (c) E. Sahin, S. Ide, M. Kurt, S. Yurdakul. *J. Mol. Struct.*, **616**, 259 (2002); (d) P.A.M. Williams, E.G. Ferrer, M.J. Correa, E.J. Baran, E.E. Castellano, O.E. Piro. *J. Chem. Crystallogr.*, **34**, 285 (2004); (e) Y. Zheng, Q. Yang, D.-J. Xu. *Acta Crystallogr.*, **E62**, m813 (2006); (f) S. Gao, L.-H. Huo, J.-W. Liu, C.-S. Gu. *Acta Crystallogr.*, **E61**, m494 (2005).
[10] J.-W. Ye, D. Li, K.-Q. Ye, Y. Liu, Y.-F. Zhao, P. Zhang. *Z. Anorg. Allg. Chem.*, **634**, 345 (2008).

[11] Z. An, R.-S. Wang. *Acta Crystallogr*., **E62**, m2493 (2006).
[12] T. Wu, D. Li, S.W. Ng. *CrystEngComm*., **7**, 514 (2005).
[13] (a) E. Terazzi, J.-M. Bénech, J.-P. Rivera, G. Bernardinelli, B. Donnio, D. Guillon, C. Piguet. *J. Chem. Soc*., *Dalton Trans*., 769 (2003); (b) F.-Y. Meng, X.-Q. Liu, S.W. Ng. *Acta Crystallogr*., **C63**, m341 (2007).
[14] S.-M. Yue, H.-B. Kan, J.-F. Ma, Z.-M. Su, Y.-H. Kan, H.-J. Zhang. *Polyhedron*, **25**, 635 (2006).
[15] M. Vrbová, P. Baran, R. Boča, H. Fuess, I. Svoboda, W. Linert, U. Schubert, P. Wiede. *Polyhedron*, **19**, 2195 (2000).
[16] X.-P. Li, M. Pan, S.-R. Zheng, Y.-R. Liu, Q.-T. He, B.-S. Kang, C.-Y. Su. *Cryst. Growth Des*., **7**, 2481 (2007).
[17] (a) L.-L. Wen, Y.-Z. Li, D.-B. Dang, Z.-F. Tian, Z.-P. Ni, Q.-J. Meng. *J. Solid State Chem*., **178**, 3336 (2005); (b) B. Xiao, H.-W. Hou, Y.-T. Fan. *J. Coord. Chem*., **62**, 1827 (2009).
[18] (a) X. Quezada-Buendía, A. Esparza-Ruiz, A. Peña-Hueso, N. Barba-Behrens, R. Contreras, A. Flores-Parra, S. Bernès, S.E. Castillo-Blum. *Inorg. Chim. Acta*, **361**, 2759 (2008); (b) M.-Y. Duan, J. Li, Y. Xi, X.-F. Lu, J.-Z. Liu, G. Mele, F.-X. Zhang. *J. Coord. Chem*., **63**, 90 (2010).
[19] M.-H. Huang, P. Liu, Y. Chen, J. Wang, Z. Liu. *J. Mol. Struct*., **788**, 211 (2006).
[20] S. Swavey, R. Swavey. *Coord. Chem. Rev*., **253**, 2627 (2009).
[21] (a) J.-P. Zou, Z.-H. Wen, Q. Peng, G.-S. Zeng, Q.-J. Xing, M.-H. Chen. *J. Coord. Chem*., **62**, 3324 (2009); (b) H. Sadeghzadeh, A. Morsali. *J. Coord. Chem*., **63**, 713 (2010); (c) X.-H. Li, Y.-P. Wang, Z.-Y. Ma, R.-L. Zhang, J.-S. Zhao. *J. Coord. Chem*., **63**, 1029 (2010); (d) Y. Yang, Y.-F. Feng, N. Liang, B.-L. Li, Y. Zhang. *J. Coord. Chem*., **62**, 3819 (2009); (e) J.-P. Zou, X.-M. Liu, L.-S. Yan, A.-M. Deng, Q.-J. Xing, M.-H. Chen. *J. Coord. Chem*., **63**, 56 (2010).
[22] A.X.S. Bruker. *SAINT Software Reference Manual*, Madison, WI (1998).
[23] G.M. Sheldrick. *SHELXTL NT, Program for Solution and Refinement of Crystal Structures (Version 5.1)*, University of Göttingen, Germany (1997).
[24] (a) Z.Y. Liu, X.G. Wang, E.C. Yang, X.J. Zhao. *Z. Anorg. Allg. Chem*., **634**, 1807 (2008); (b) K. Nakamoto. *Infrared and Raman Spectra of Inorganic and Coordination Compounds*, Wiley, New York (1997).
[25] Y.-X. Yang, Y.-K. Yang, T.-C. Zhao, Y.-Y. Huang, D.-H. Wang, W.-Z. Chen. *Acta Photon. Sin*., **31**, 1273 (2002).
[26] X.-Y. Li, H.-J. Sun, D.-F. Sun. *Acta Chim. Sin*., **53**, 336 (1995).
[27] C. Piguet, J.-C.G. Bünzli, G. Bernardinelli, G. Hopfgartner, A.F. Williams. *J. Am. Chem. Soc*., **115**, 8197 (1993).
[28] P.-J. Jiang, Z.-J. Guo. *Coord. Chem. Rev*., **248**, 205 (2004).
[29] E.-C. Yang, Y.-N. Chan, H. Liu, Z.-C. Wang, X.-J. Zhao. *Cryst. Growth Des*., **9**, 4933 (2009).